Photo-Configurable, Cell-Remodelable Disulfide Crosslinked Hyaluronic Acid Hydrogels

Linke Wu[a, b], *Stefania Di Cio*[a, b], *Helena S. Azevedo*[a, b], *Julien E. Gautrot*[a, b*]

[a] Institute of Bioengineering and [b] School of Engineering and Materials Science, Queen Mary, University of London, Mile End Road, London, E1 4NS, UK.

* To whom correspondence should be addressed. E-mail: j.gautrot@qmul.ac.uk

Abstract

Dynamic photo-responsive synthetic hydrogels offer important advantages for biomaterials design, from the ability to cure hydrogels and encapsulate cells *in situ* to the light-mediated control of cell spreading and tissue formation. We report the facile and effective photo-curing and photo-remodelling of disulfide-crosslinked hyaluronic acid hydrogels, based on photo-oxidation of corresponding thiol residues and their radical-mediated photo-degradation. We find that the mechanical properties of disulfide hydrogels and the extent of their photo-remodelling can be tuned by controlling the photo-oxidation and photo-degradation reactions, respectively. This enables the photo-patterning of the mechanical properties of hydrogels, but also their self-healing and photo-mediated healing. Finally, we demonstrate the ability to encapsulate mesenchymal stromal cells within these materials and to regulate their protrusion and spreading in 3D matrices by controlling the mechanical properties of the disulfide networks. Therefore, synthetically accessible photo-configurable disulfide hydrogels offer interesting opportunities for the design of soft biomaterials and the regulation of cell encapsulation and matrix remodelling for tissue engineering.

Introduction

Synthetic hydrogels have emerged as an important class of biomaterials to promote tissue regeneration and mimic the extra-cellular matrix (ECM) for the design of advanced in vitro models[1, 2]. They allow to capture the biochemistry of cell adhesive proteins, the presentation of growth factors and the mimicking of important ligands regulating cell signalling[3]. Hydrogels also allow the regulation of the mechanical properties of the ECM and its degradability by cells, as they remodel their environment[4, 5]. Hence they are increasingly used in strategies promoting tissue repair and providing a microenvironment regulating the formation of organotypics and organoids *in vitro*[6, 7].

Although cell adhesion to a wide range of hydrogels has been studied, cell encapsulation, degradation and spreading within 3D hydrogels is restricted to a much narrower range of cure chemistries. Indeed, cytocompatible chemistries have to be used to encapsulate cells in hydrogels, amongst which the most popular are Michael addition-based[8-10], alkyne-azide click[11, 12] and radical thiol-ene/yne click chemistries[13-15]. These coupling strategies enable efficient network formation, relatively fast (seconds to minutes), in air and without the use of cytotoxic catalysts or coupling agents. They also allow a wide range of polymer architecture to be introduced, with polymer backbones such as multi-arm poly(ethylene glycols) (PEG)[13, 16], gelatin[17] and dextran[18], and crosslinkers like poly(ethylene glycol)[19] and short peptide sequences[8, 15]. The glycosaminoglycan hyaluronic acid (HA) has also attracted considerable attention as a scaffold polymer[20, 21], owing to the relative simplicity of its functionalisation, its availability in a range of molecular weights and its inherent biocompatability. For example, functionalised HA chains can be crosslinked via acrylate or enzymatically cleavable peptides, to afford non-degradable and cell remodellable hydrogels, respectively[5]. The introduction of further moieties enabling supramolecular interactions can also tailor the viscoelastic profile of associated hydrogels[22]. Thiolated HA has also been crosslinked with methacrylated HA, via a photo-radical thiol-ene mechanism, enabling curing with blue light in a 2-5 min[23]. Alternatively, S-protected thiolated HA has been shown to spontaneously crosslink in the presence of small concentration of thiols (endogenous or added to trigger gelation)[24].

In addition to the simple formation of a polymer network, hydrogels have been designed to enable their controlled remodelling via photo-controlled reactions. Hence sequential thiol-ene radical chemistry allows the control of matrix stiffening, which in turn may impact on cell morphology and phenotype[5, 15]. An interesting additional feature is the design of photo-degradable hydrogels, mainly

based on nitrobenzyl moieties introduced within the crosslinking groups regulating network formation[12, 25]. Such light-remodelable materials allow the control of adherent cell niches in 3D hydrogels and enable the control of their migration in 3D matrices[3]. However, the synthesis of these matrices remains synthetically challenging and relatively difficult to implement in biology laboratories. Tools that simplify the design of remodelable hydrogels are therefore appealing.

During the formation of thiol-ene based hydrogels (Michael addition or radical-mediated), the use of thiolated polymer backbones can lead to uncontrolled gelation via oxidation and formation of disulfide networks, depending on pH[26]. Hence radical-based thiol-ene coupling of non-activated alkene-functionalised polymer backbone (e.g. with dicysteine peptides) offers the advantage of a stable formulation selectively triggered by photo-irradiation. Disulfide-based hydrogels and biomaterials have attracted attention for the design of gene delivery vectors and drug delivery biomaterials[27, 28]. A few reports have proposed the formation of disulfide-based hydrogels generated via oxidation of corresponding thiolated backbones[29], in some cases at physiological pH[30, 31]. Although the photo-oxidation of thiol moieties has been recently proposed for the functionalisation of biointerfaces[32], the light-mediated gelation of such disulfide networks has not been reported to date.

Here we report the design of a simple and accessible strategy to generate light- and cell-degradable hydrogels based on disulfide networks. We report that photo-initiation of radicals can effectively control the crosslinking of thiolated hyaluronic acid hydrogels and enable the control of their mechanical properties. In addition, we demonstrate that this strategy can be extended to the simple photo-degradation of the hydrogel network, whilst only requiring simple, accessible thiolated scaffolds. We also report that these materials display self-healing properties and can be remodelled by small-molecule thiols. We propose that this phenomenon forms the basis of their cell-mediated degradability and demonstrate the ability of these hydrogels to regulate cell spreading in 3D synthetic matrices.

Experimental Section

Unless otherwise stated, all experiments were carried out at room temperature (in our laboratories, 20°C). The pH of all hydrogel precursor solutions was systematically measured and set to 7.4, using a Mettler Toledo pH meter set up with an LE438 pH electrode, unless otherwise stated. Substitution degrees refer to the number of disaccharide repeats functionalised with thiol residues.

Materials. Sodium hyaluronate (HA, MW 150 to 300 kDa) was purchased from Lifecore Biomedical. Cystamine dihydrochloride (CS), N-hydroxysuccinimide (NHS), phosphate buffer saline (PBS) tablets, Dulbecco's PBS, *N*-(3-dimethyl aminopropyl)-*N*′-ethylcarbodiimide hydrochloride (EDC), 1-hydroxybenzotriazole hydrate (HoBt) , dithiothreitol (DTT) , 5,5′-dithiobis(2-nitrobenzoic acid) (DTNB), N-ethylmaleimide (NEM), glutathione (GSH), oxidized glutathione (GSSG), cell viability live/dead kit and 2-Hydroxy-4′-(2-hydroxyethoxy)-2-methylpropiophenone (I 2959) were obtained from Sigma-Aldrich. The cysteine functional RGD peptide GCGYGRGDSPG was purchased from Proteogenix, France and trifluoroacetate (TFA) was removed by solid phase extraction (PL-HCO_3 MP SPE tube). The GCG sequence of this peptide was selected based on the increased pKa of the corresponding cysteine, enabling improved thiyl formation efficiency at neutral pH[14]. Other chemicals were used directly after received.

Synthesis of thiolated HA (HA-SH). HA-SH was synthesised following a protocol adapted from the literature[26]. In brief, 500 mg HA (corresponding to 1.5 mmol of thiols) was dissolved in 150 mL deionized water and 255 mg HOBt (1.88 mmol) were added to this solution, together with cysteamine (450 mg, 1.88 mmol). The pH value of the solution was adjusted to 4.7 after complete dissolution. EDC (115 mg, 0.6 mmol) was added in 3 batches at 20 min intervals. After 24 h reaction, the pH value was raised to 9, followed by the addition of DTT (385.5 mg, 2.5 mmol). After reacting for a further 24 h, the products were purified by dialysis in acidic conditions (pH 4, adjusted via addition of 1 M HCl) for 3 days and deionised water for 2 days. The solution was subsequently frozen and lyophilized. The purity and functionalisation (substitution degree, SD) level of HA-SH were determined by ^{1}H NMR (using a Bruker AVIII 400; in D_2O). The quantification of free thiols on the side chains of HA-SH was also carried out by a modified Ellman's assay to determine SD (Supplementary Figure S4). Both methods led to an SD of 16 ± 2.3%.

Photo-curing and –degradation of disulfide crosslinked HA hydrogels. HA-SH solutions (1.25 wt% to 5 wt%, corresponding to thiol concentrations of 4.9 to 19.5 mM, in PBS) were irradiated in the presence of the radical photo-initiator Irgacure 2959 (I2959; concentrations of 0.24 to 3.91 mM). I2959 stock solutions (0.26 mM in methanol; depending on concentrations required, the volumes of stock solutions injected corresponded to 0.1 to 7.6 μL) were added to HA-SH PBS solutions (100 μL) followed by 2 to 10 min UV irradiation (Omnicure series 2000, 320 to 500 nm band, intensity to 17 mW/cm^2, calibrated with an ILT 1400-A radiometer).

Photo-rheology. Rheological measurements were performed on a hybrid rheometer (DHR-3) from TA Instruments fitted with a UV accessory. Solutions were introduced between an upper parallel plate (20 mm, lowered onto the solution) and a bottom quartz window (allowing transmittance of UV light). UV irradiation (Omnicure S1500 mercury lamp, λ 280–600 nm, connected via a light guide; calibration using an ILT 1400-A radiometer; 17 mW/cm^2 unless otherwise specified) was started after a period of oscillation (30 s) to equilibrate the system. The rheological characterisation and light curing procedure was controlled by the TRIOS software. Oscillations were set in controlled strain mode at 0.4% strain, which was found to be within the linear viscoelastic region of the hydrogels generated, determined from initial frequency and strain sweeps. The UV-curable mixture was sandwiched between two plates of the rheometer at a fixed gap of 250 μm while the axial force was controlled with a deviation of less than 0.1 N during the measurement. For in situ monitoring of the progression of cross-linking, we carried out time sweeps (10 min) with fast sampling mode of 25 Hz, to allow monitoring of the rapid rates of reaction. Frequency sweep measurements (0.4% strain) were conducted before and after the UV cure to examine the change in rheological behaviour. Stress relaxation experiments and strain sweeps were carried out after UV curing (and frequency sweeps), 2.0% strain was reached in 2 s and held for 180 s. All experiments were repeated in triplicate for each composition or condition.

Liquid Chromatography-Mass Spectrometry (LC-MS). Thiol and disulphide photo-reactivity was characterised by LC-MS, using glutathione and oxidised glutathione as model compounds. In order to distinguish GSH and GSSG via LC-MS, we reacted free thiol GSH with NEM. For calibration, freshly prepared 20 mM GSH solutions in degassed water (GSH, 6.1 mg ml^{-1}) were diluted to 0, 80, 120, 250, 500 and 1000 μM in deionised water. In each 470 μL aliquote, 30 μL of NEM solution (3.88 g of NEM in 100 mL) were added and allowed to react for 5 min at room temperature. Finally,

500 μL of deionised water were added to this mixture, diluted 20 times prior to analysis. For the calibration of oxidised glutathione, 10 mM GSSG was prepared in water (24.5 mg of GSSG in 4 mL of water). For calibration, the stock solution was diluted to 40, 80, 120, 250, 500 and 1000 μM. In each 500 μL solution, 500 μL of deionised water were added to make up final standard solutions and diluted 20 times prior to analysis. Photo-disulfide formation and cleavage were carried out. 10%, 25%, 50%, 75% and 100% of PI (mol% vs. thiols) were added to 470 μL GSH (1 mM) solutions. The mixtures were cured by UV irradiation (17 mW/cm^2) for 2 to 6 min. After reaction, 30 μL of NEM solution were added and allowed to react for 5 min at room temperature. 500 μL of deionised water were added to this mixture, diluted 20 times prior to analysis. For photo-cleavage of disulfides, 50%, 100% 200% and 400% of PI (mol% with respect to sulfur atoms) were added to 500 μL GSSG (1 mM) solutions. The mixtures were cured via UV irradiation (17 mW/cm^2) for 2 to 6 min. 30 μL of NEM solution were added and allowed to react for 5 min at room temperature. 500 μL of deionised water were added to this mixture, diluted 20 times prior to analysis.

For liquid chromatography, the mobile phase A was prepared using 0.01% (vol/vol) formic acid in HPLC-grade water. Mobile phase B was 0.01% formic acid in acetonitrile. Chromatographic separation was performed on a Waters BEH system equipped with a C18 column (1.7 μm, 50 mm) and detection was performed with an MS (Waters Synapt G2Si HDMS). The mobile phase B (100%) was first run at 1.25 mL min^{-1} for at least 5 min to equilibrate the column (at a temperature of 25 °C). The mobile phase composition was gradually changed to 60% phase A and 40% phase B with a flow rate of 0.4 mL min^{-1}. For each repeat of this experiment, we ran one or more blanks followed by standards and reaction samples under isocratic conditions. At the end of the run, the column was flushed with 100% phase B for 2 min and the system was then re-equilibrated to the initial isocratic conditions, prior to the next injection.

Mechanical Characterisation by atomic force microscopy (AFM) nano-indentation. An NT-MDT Ntegra AFM was used for AFM nano-indentation. Bruker 8–10 contact cantilever with pyramidal tips were used (spring constant was calibrated, 0.69 N/m). The cantilevers were calibrated by doing initial indentations and topography scanning on a silicon wafer. Each gel sample was soaked in PBS to perform wet AFM and testing was carried out via a 10×10 grid of indentations at three different locations on three different samples for each formulation. The indentation curves were then analysed using a custom made MATLAB script using the Oliver-Pharr model[33].

Tensile testing. 10 wt% HA-SH hydrogels were prepared for characterisation of tensile properties and self-healing. Samples (formed in Teflon molds) were cured with 5 mol% of initiator for 1 min. Mechanical testing was carried out with an Instron frame equipped with a 5 N load cell. Rectangular samples (4.9 × 8.3 mm, with a thickness of 1.1 mm; determined with a calliper) were used and measurements were carried out in triplicate. Measurements were carried out at room temperature at a constant strain rate of 1 mm/mm/min. The initial region of low extension (0–10%) in the stress–strain plot was used to determine the tensile properties of samples.

Mesenchymal stem cells culture and 3D encapsulation. Human bone marrow derived mesenchymal stem cells (hMSCs) were obtained from PromoCell and cultured on T75 flasks in hMSC growth medium (PromoCell). hMSCs were harvested with 5 mL accutase-solution (PromoCell), centrifuged, counted and re-suspended in PBS at the desired density. For cell encapsulation, 5 wt% HA-SH sterile solutions were prepared (HA-SH was sterilised as a powder via 15 min UV treatment prior to reconstitution of solutions in sterile conditions) and cells in PBS were seeded at a cell density of 2.0M cells/mL to make suspensions in HA-SH solution with final concentrations of 2.5 wt% and 1.25 wt%. The final cell density was 1.0M cells/mL. PI stock solution was prepared in 70% ethanol (58 mg/mL). The volume (and therefore stoichiometry) of PI solution was varied to control the mechanical properties of hydrogels. The resulting solutions were pipetted into a 48-well plate and cured under UV (17 mW/cm^2) for 2 min. The PBS solution was replaced by medium prior to culture in growth medium for 48 h.

Cell staining and imaging. The viability of hMSCs in HA hydrogels was determined using a Live/Dead viability/cytotoxicity assay. In brief, encapsulated hMSCs were incubated in serum free PBS with 2 μM Calcein AM, 4 μM ethidium homodimer-1 for 20 min at 37 ^{o}C. The gel samples were rinsed three times with PBS and stained cells were imaged using a DMI8 Leica epifluorescence microscope. The percentage of viable cells was calculated by counting the number of live cells divided by the total number of cells. For cytoskeletal and matrix deposition stainings, cells were fixed and permeabilized simultaneously in 4% PFA and 0.2% TritonX100, blocked for 1 h in 4% BSA. Stock solutions of phalloidin (1: 500) were prepared by dissolving 1 mg phalloidin–tetramethylrhodamine B isothiocyanate (Sigma-Aldrich) in 300 μL methanol (VWR chemicals). Dapi solutions (stock concentration: 5mM, 1:1000) were prepared by dissolving 5 mg 4',6-diamidino-2-phenylindole dihydrochloride (Sigma-Aldrich) in 1750 μL dd H_2O. Primary antibodies (anti-

fibronectin (1:1000), Sigma Aldrich) were diluted in PBS containing 4% BSA and hydrogels were stained at 4 °C overnight. Secondary antibodies conjugated to AlexaFluor 488 (ThermoFisher Scientific, 1:1000 in 4% BSA) were used for immunofluorescence staining. For F-actin staining and Dapi staining, rhodamine-conjugated phalloidin and Dapi were added with the secondary antibodies and incubated for 1h at room temperature. Hydrogels were washed. All washing steps were carried out by diluting with PBS 6 times. When adding reagents, half of the liquid covering the samples was removed and replaced with double concentrated reagent solutions.

Statistical analysis. Statistical comparisons between two experimental groups were performed using two-tailed Student's t-tests and comparisons among more groups were performed using one-way or two-way ANOVA with Bonferroni post hoc testing.

Results and Discussion

Rapid photocuring of thiolated hydrogels. Thiolated HA (HA-SH, degree of substitution of 16 ± 2.3%, see Supplementary Figure S1) was found to rapidly gel upon irradiation in the presence of the radical photoinitiator Irgacure 2959 (Figure 1), in the absence of any olefinic crosslinker. Gelation was not observed in the absence of initiator (but with photo-irradiation) and samples cured in the presence Lithium phenyl-2,4,6-trimethylbenzoylphosphinate (LAP) also gelled (results not shown). Examination of cure rates by photo-rheology indicated that the shear moduli rapidly increased following the start of irradiation (Figure 1 and Supplementary Figure S2), with moderate inhibition (a delay in the onset of increase of the storage modulus ranging from 7 to 11 s when the photoinitiator concentration was varied between 5 and 20 mole%), in line with the rapid transfer of radical to thiol moieties. Therefore, the phenomenon observed displayed the hallmarks of a radical-mediated photo-oxidation of thiols into disulfide. Consistent with this hypothesis, the degree of crosslinking and shear storage modulus of resulting hydrogels increased as a function of photoinitiator concentration (Figure 1B). In addition, upon treatment with the strong reducing agent dithiothreitol (DTT), re-dissolution of the hydrogel formed was observed (Figure 1A and C). Together, these results indicate that photoinitiation of free radical leads to the formation of thiyl radicals that can recombine to form disulfide bonds, leading to the crosslink of HA chains.

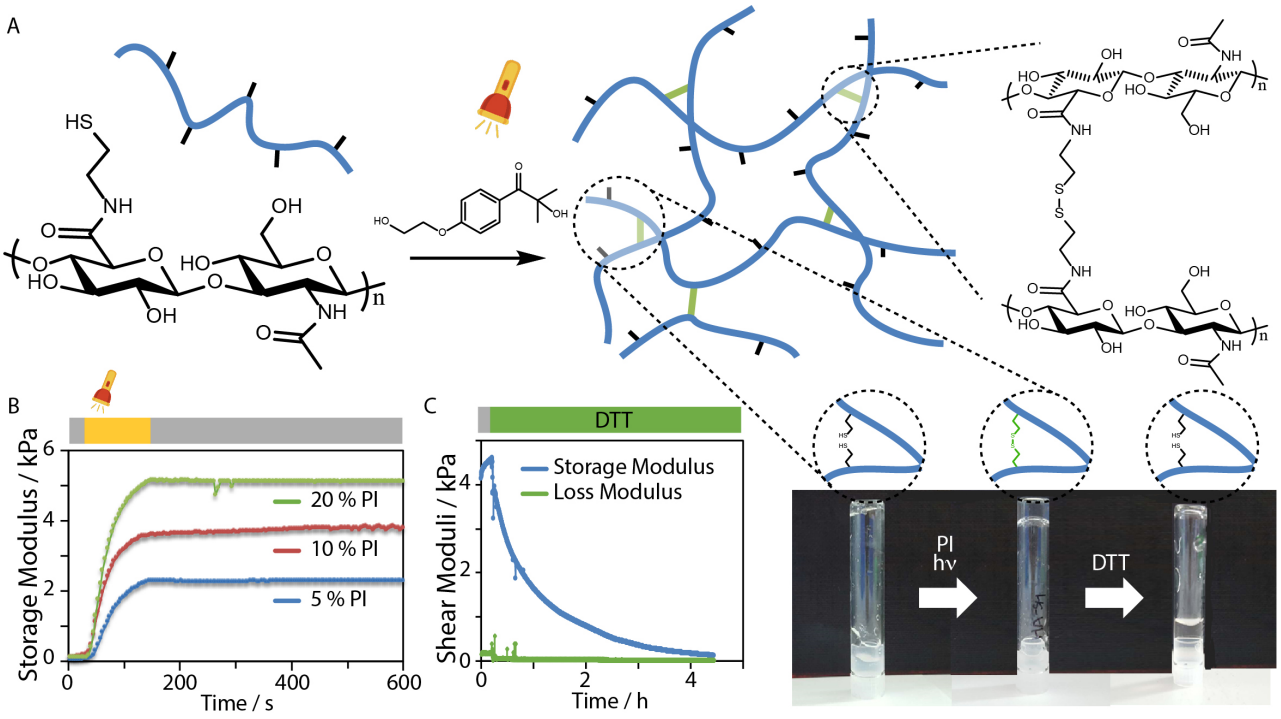

Figure 1. A. HA-SH crosslinked via photo-oxidation in the presence of PI (I2959). Images on the right illustrate the gelation of the HA solution, followed by the degradation of the resulting gel upon DTT treatment (10 mg/mL, pH 9.0, 2 h). **B.** Oscillating time sweeps (1 Hz, 0.4% strain) recorded during the gelation of 5 wt% HA-SH with different percentages of PI (17 mW/cm^2 light intensity from 30 to 150 s; mol% of PI are compared to the thiol content). **C.** Oscillating time sweep of 5 wt% HA-SH hydrogel (crosslinked with 10 mol% PI, with respect to thiol content) during incubation in a DTT solution (10 mg/mL, pH 9.0).

To explore the mechanism of hydrogel formation and the efficiency of photo-oxidation of thiol moieties, we investigated a model reaction with glutathione (GSH) via liquid chromatography-mass spectrometry (LC-MS, Figure 2A). As reduced and oxidized GSH both elute at identical time by LC, we allowed free thiol groups to react with N-ethylmaleimide (NEM) prior to calibration and characterization (Supplementary Figure S3). Upon irradiation of GSH in the presence of I2959 photoinitiator (PI), we observed the gradual disappearance of free GSH (Figure 2B and C; note the presence of two peaks corresponding to the two diastereoisomers of NEM-reacted GSH). This was also confirmed via an Ellman's assay (Supplementary Figure S4). In the absence of photonitiator, irradiation did not lead to the formation of any product or the disappearance of any starting material. Interestingly, although the decomposition of I2959 upon photo-irradiation results in the formation of

two radicals, we only observed 92 ± 5.7% and 64 ± 8.9% reactivity at thiol/PI ratios of 1 and 0.5, respectively. Although incomplete PI conversion was observed at higher ratios, this suggests both radicals generated are not equally efficient for transfer to the thiol moieties and may be involved in recombinations. At lower thiol/PI ratios, higher GSH conversions were observed, perhaps implying the impact of carbon radical recombinations at higher ratios. However, we could not detect traces of such recombination by LC-MS and only detected the benzoyl radical degradation product. This is perhaps a result of the high stability of the tertiary radical second fragment generated during the decomposition of I2959.

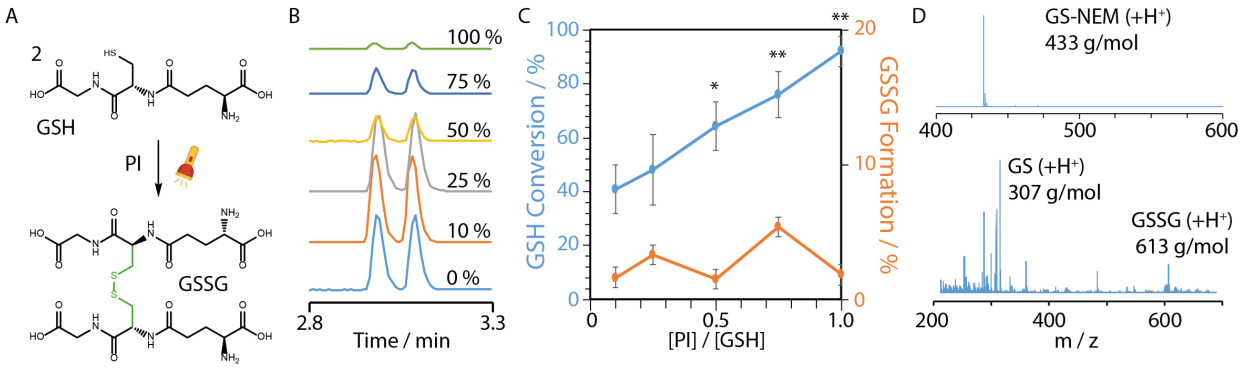

Figure 2. A. Photo-oxidation of glutathione (GSH) to oxidised glutathione (GSSG). **B.** LC-MS is used to determine the ratio of converted GSH and formed GSSG at different PI concentrations (mole% vs thiols). **C.** Corresponding quantification. Statistical analysis reported for comparison of corresponding condition with [PI]/[GSH] of 10%. *, $p < 0.05$; **, $p < 0.01$. **D.** Mass spectra of GS-NEM and GSSG formed by photo-oxidation.

Analysis of the mass of the molecules corresponding to the peak of GSH (reacted with NEM) confirmed the expected structure and LC-MS also confirmed that oxidized glutathione was formed during photo-irradiation in the presence of PI (Figure 2D). The conversions achieved remained relatively low, however, typically below 10% after 2 min photo-irradiation at ratios of PI/thiol below 1.0, and only reaching 13.8% after 4 min irradiation, without significant further increase thereafter (Supplementary Figure S5). The formation of thioester benzoate side-products, identified in the mass spectrograms of the peak at 4.5 min, may explain the low level of disulfides formed. Despite these modest conversions, rapid gelation was observed for the crosslinking of thiolated HA. This is proposed to be due to the high molecular weight of the HA chains used (200 kDa) and the high

functionalization level achieved (16 ± 2.3%), corresponding to 80 thiol moieties per chains, on average. For such high degree of functionalization, conversions to disulfides of c.a. 10% remain sufficient to induce network formation, as corresponding to 8 crosslinks per chain on average. Therefore, considering the high molecular weight of the HA chains used, a rapid formation of insoluble networks is expected. This is consistent with the rapid increase in viscosity and shear moduli observed by photo-rheology.

Photo-remodeling of disulfide hydrogels. Initial results clearly indicated that the crosslinking density in the photo-disulfide curing of HA hydrogels was regulated by the PI concentration, with respect to thiol moieties. Another strategy typically used to tune the mechanical properties of hydrogels is the control of the polymer or monomer density[34]. Indeed, we found that the shear modulus of thiolated hydrogels was reduced by nearly 1 order of magnitude when the polymer concentration was reduced to 2.5 wt% (compare Figure 3 to Figure 2). However, we also observed that as the concentration of PI was increased over a wider range, the evolution of the modulus did not progress as expected. Whereas we noted an initial increase in storage modulus, as the PI/thiol ratio increased above 10%, the initial rate of curing increased, but was then followed by a decrease in modulus at longer cure times. This was proposed to be due to scission of disulfide bonds by further radicals generated during the reaction (Figures 3A and B). This effect was so pronounced that at large excesses of PI, the gel disrupted almost completely.

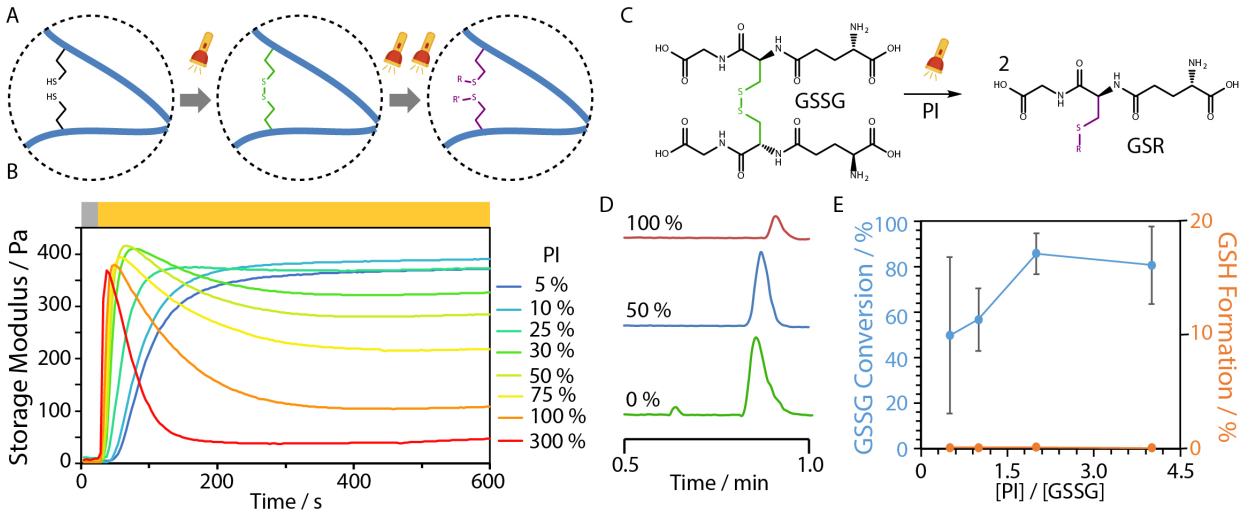

Figure 3. Controlled degradation of photo-crosslinked HA hydrogels. A. Successive photo-oxidation and photo-degradation of HA-SH hydrogels. **B.** Oscillating time sweeps (1 Hz, 0.4% strain) of the crosslinking and subsequent photo-degradation of 1.25 wt% HA-SH hydrogels at different PI concentrations (mole% with respect to thiols are indicated; UV, 17 mW/cm^2 light intensity, on between 30 and 600 s). **C.** Photo-cleavage of GSSG. **D.** LC-MS characterisation of the conversion of GSSG at different PI concentrations. **E.** Corresponding quantification of GSSG conversion and GSH formation.

To gain further insight into the mechanism of photo-cleavage of disulfide HA hydrogels, we carried out cleavage reactions on oxidised glutathione (GSSG, Figure 3C) and monitored the progress via LC-MS (Figures 3D and E). We observed a gradual disappearance in GSSG peaks as the concentration of PI increased, reaching > 80% at PI/GSSG ratios above 2.0. Such high degrees of cleavage were already achieved after 2 min of irradiation and slightly increased at higher reaction times (Supplementary Figure S5C). However, at all concentrations and reaction times tested, we could not detect the formation of any free GSH (Figure 3E), indicating that cleaved disulfide and associated thiyl radicals recombined with other species present in the environment. Indeed, we detected the formation of thioesters (specifically, phenyl thioesters) during this reaction (identified by LC-MS).

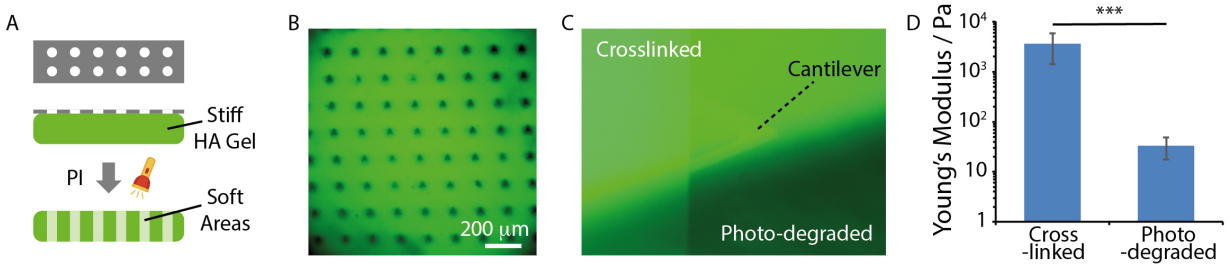

Figure 4. A and B. Photo-patterning of crosslinked 5 wt% HA-SH hydrogels (100 mole% PI vs. thiol, 30 s UV curing, 17 mW/cm^2 light intensity) by 300 s UV curing through a photo-mask. **C.** Microscopy image recorded during AFM indentation on a patterned 5wt% HA-SH hydrogel, showing the interface between irradiated and non-exposed areas and the position of the AFM cantilever. **D.** Young's moduli measured by AFM indentation in non-exposed (crosslinked) and photo-degraded areas. ***, $p < 0.001$.

The photo-degradation of hydrogels is of particular interest in the field of bioengineering[35], as a tool to modulate the mechanical properties of hydrogels[36] and enable to spatially regulate the differentiation of stem cells[3] and their motility[12]. Typically, the design of these materials is based on the incorporation of nitrobenzyl moieties that fragment upon photo-irradiation. These materials remain relatively difficult to access and synthesise and not widely used in the field of bioengineering, despite their important potential. Therefore, we next explored whether the accessible disulfide-based hydrogels developed could be remodelled upon photo-irradiation, to display patterns of areas with controlled mechanical properties. A disulfide hydrogel was photo-patterned through a mask, after infiltration of additional photoinitiator (Figure 4A). This resulted in the generation of soft gel areas embedded within the stiffer initial gel matrix (Figure 4B). The associated change in local modulus was confirmed by AFM indentation of crosslinked and photo-degraded areas (Figure 4C and D).

Self-healing disulfide hydrogels. The reversible formation of bonds is an important strategy to confer self-healing properties to materials. Typically, rapid self-healing relies on supramolecular bonding[37] as covalent bonding requires longer healing times. Self-healing biomaterials may be of interest in the field of regenerative medicine, for example for applications in which biomaterials are exposed to relatively challenging mechanical stimulations (such as hydrogels for epicardial

placement or cartilage repair). Considering the rapid crosslinking observed in our disulfide hydrogels, we explored their self-healing properties. Indeed, disulfide-crosslinked polymer networks and hydrogels have been reported to display self-healing properties, via a disulfide metathesis mechanism[38, 39]. We carried uniaxial stretch of thiolated HA hydrogels (10 wt%) and observed failure near 100% strains (Figure 5). The fractured samples were then placed in direct contact, coated with a PI solution (3.9 mM), and photo-irradiated (120 s) whilst maintaining physical contact between the samples (Figure 5A). This led to effective healing of the samples, which displayed sufficient mechanical integrity for free handling. Following this step, uniaxial stretching was repeated. We observed a slight increase in the Young's modulus of the healed materials, although failure occurred at reduced ultimate stress than for pristine samples (Figures 5B and C). This process could be repeated and we observed further stiffening of the sample in the second round of healing. The stiffening effect is proposed to be associated with the further crosslinking of the networks, as the interface was allowed to heal under photo-irradiation. However, defects, especially at the edge of the samples limited the full recovery of mechanical performance.

Considering the observed stiffening effect, we explored whether direct disulfide exchange and thiol oxidation at the interface of the failed samples could be sufficient to induce healing. Failed samples were placed in direct contact and maintained in position using parafilm and a glass slide, for 24 h at room temperature (20^{o}C). Following this process, we observed that the mechanical integrity of the samples was sufficient for mechanical characterisation and carried out subsequent uniaxial stretch (Figure 5). Similarly, to what was observed with the photo-induced self-healing of samples, the ultimate strength of the healed samples was reduced, however the Young's modulus of the materials generated was identical to that of the pristine samples, consistent with the notion that further photo-irradiation induced stiffening of the samples.

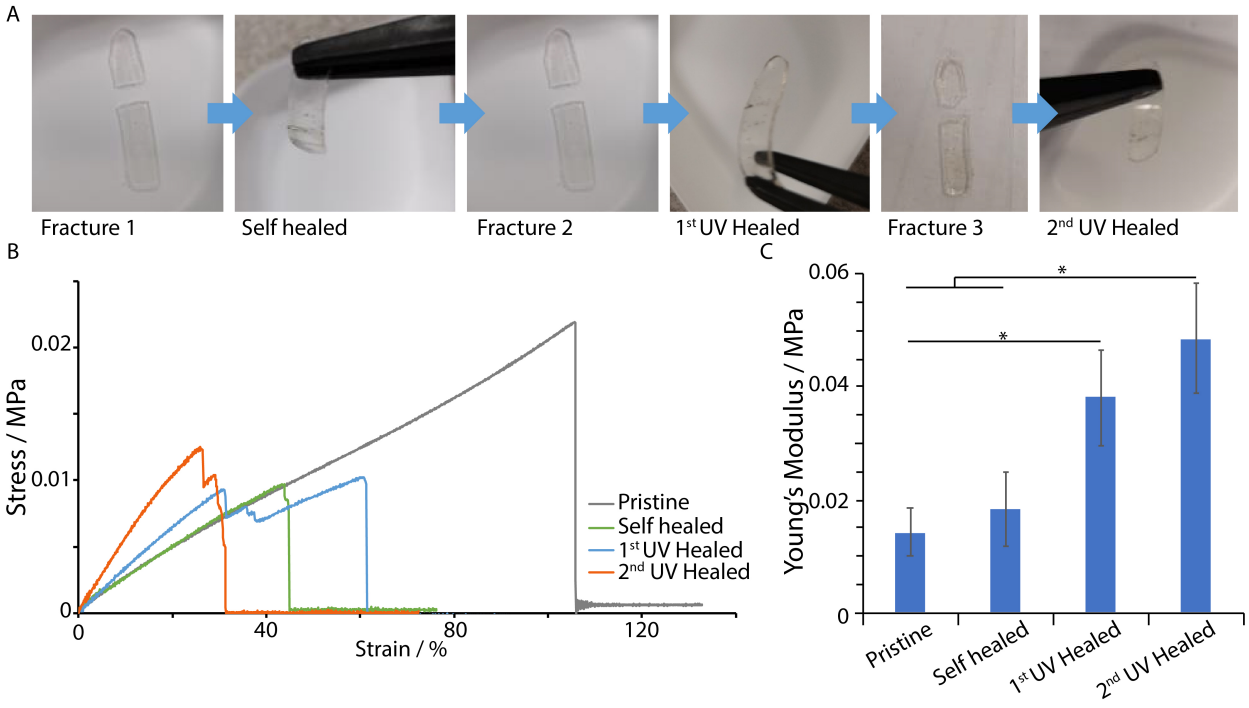

Figure 5. A. Images displaying HA-SH hydrogels before and after fracture, following by self-healing (in the absence of additional photo-curing, or aided by photo-irradiation). **B.** Stress–strain curves of HA-SH hydrogels (10 wt%) before and after self-healing. For UV healed samples, a 0.25 mM PI solution was applied, followed by UV irradiation (17 mW/cm^2 intensity) for 2 min. **C.** Corresponding Young's moduli (derived from data up to 10 % strains). Error bars are standard errors, from independent triplicates. *, $p < 0.05$.

Cell-remodelable disulfide hydrogels. The ability of disulfide networks to spontaneously heal following failure indicated that thiol-disulfide exchanges could play an important role in their remodelling. This led us to investigate whether physiologically relevant thiol molecules may be able to degrade disulfide hydrogels. Glutathione (GSH) is a low molecular weight thiol compound produced by cells and that plays a role in the regulation of oxidative stress. It is present at concentrations ranging from 0.01 mM extracellularly to 1-10 mM in the cytoplasm[40]. We first tested whether GSH would be sufficient to induce the degradation of photo-induced disulfide HA hydrogels (Figures 6A and B; Supplementary Figure S6). Following photo-crosslinking, hydrogels were incubated in a GSH solution (10 mM) for up to 2 days. During this time, we observed a significant reduction in their Young's modulus, from 42 ± 4 kPa to 16 ± 2 kPa. In comparison, hydrogels that were simply incubated in PBS did not display a significant softening, although swelling following on from gelation induced some reduction in their Youngs' modulus (Figure 6A; note that the modulus

may not necessarily have reached a minimum, but was significantly reduced in the presence of free GSH, at identical incubation time). The initial modulus obtained just after crosslinking (42 kPa) is higher than the modulus that would be approximated from Figure 1 (near 20 kPa, assuming a Poisson ration of 0.5). We attribute this to some level of tip-gel adhesion, resulting in an increase in actual contact with the probe, as previously studied in the case of poly(acrylamide) gels and soft silicone substrates[34]. In addition, upon incubating the glutathione-partially degraded in PBS solutions, we observed the partial recovery of disulfide hydrogels and some restauration of their modulus (Figure 6A). Together, our results demonstrate that disulfide photo-crosslinked hydrogels can be remodelled by free thiol molecules, but that such process is reversible (Figure 6B), therefore constituting a viable mechanism for the remodelling of hydrogels by cells encapsulated in these materials.

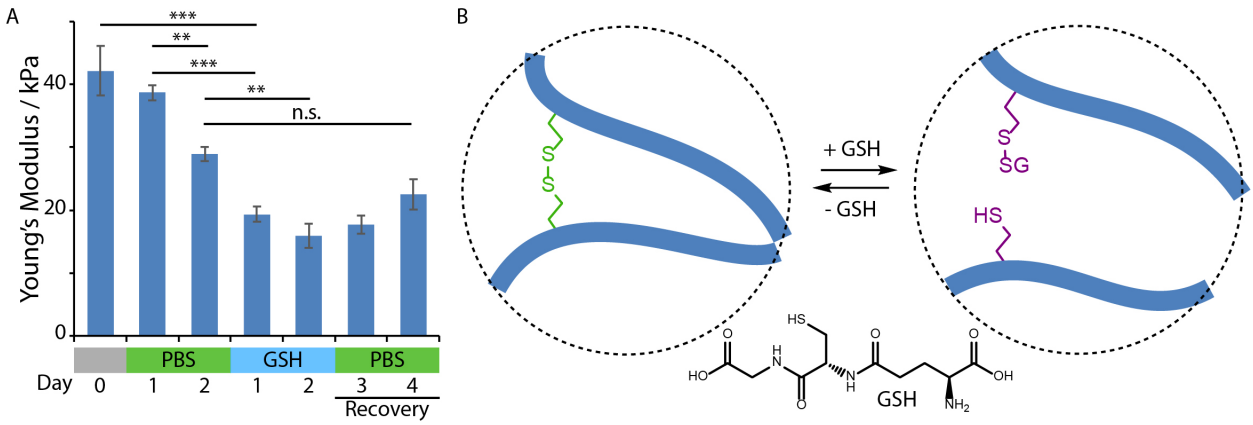

Figure 6. A. AFM nanoindentation was performed on 5 wt% HA-SH hydrogels before and after incubation in PBS (crosslinked with 25 % PI), followed by incubation in 10 mM GSH in PBS solutions and finally washed and incubated in PBS again. n.s., not significant; **, $p < 0.01$; ***, $p < 0.001$. **B.** Proposed mechanism for GSH-mediated degradation (thiol-disulfide metathesis) and recovery.

Considering the striking impact that hydrogel stiffness and degradability plays on cell spreading and phenotype in 3D matrices[1, 5, 41], we next identified a series of disulfide crosslinked HA hydrogels displaying controlled mechanical properties (Figures 7 A and B; Supplementary Figure S7). Via a combination of varied polymer content and crosslinking density (via the variation of PI concentrations), we achieved the formation of hydrogels with shear moduli in the range of 260 ± 59 to 1052 ± 152 Pa, a range in which hydrogel stiffness is typically associated with changes in cell phenotypes in 3D matrices[1]. To examine the impact of HA-SH hydrogel stiffness on cell spreading, human bone-marrow derived mesenchymal stem cells (hMSCs) were seeded within the resulting photo-crosslinked disulfide hydrogels and their spreading monitored within 48 h. High cell viabilities were observed within the range of hydrogels tested (Supplementary Figure 8), consistently with the low impact of irradiation conditions on cell phenotype[42]. As the crosslinking density and associated Young's modulus of the hydrogels increased, we observed a clear restriction in cell spreading (Figure 7 C and D and Supplementary Figure 9). Whereas cells in 1050 Pa remained mainly rounded, cells in more compliant disulfide hydrogels gradually spread and elongated, ultimately adopting morphologies comparable to those of cells spreading within fibrin hydrogels[43].

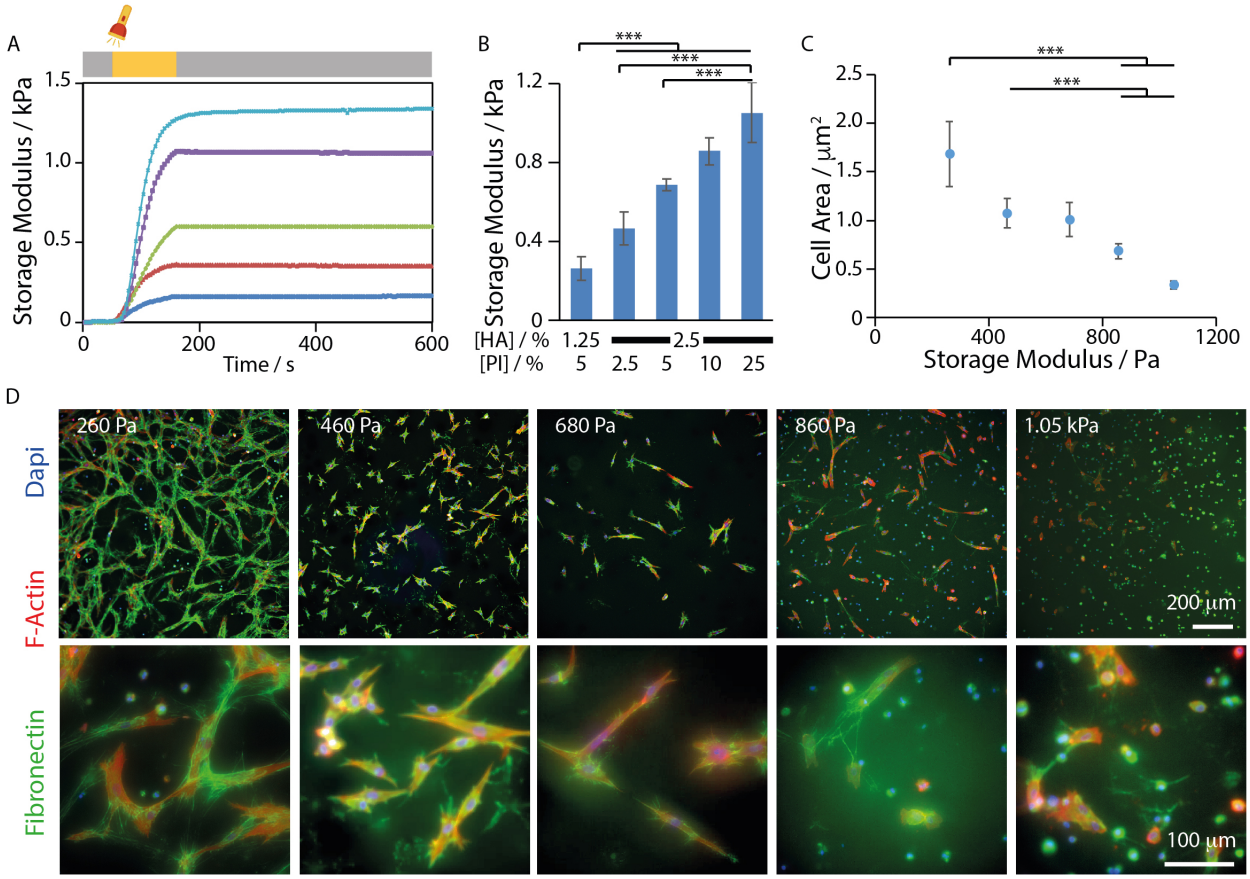

Figure 7. A. Control of mechanical properties of photo-crosslinked HA-SH hydrogels via polymer and PI concentrations (dark blue, 1.25wt% HA-SH with 5 mol% PI; red, 2.5 wt% HA-SH with 2.5 mol% PI; green, 2.5 wt% HA-SH with 5 mol% PI; purple, 2.5 wt% HA-SH with 10 mol% PI; turquoise, 2.5 wt% HA-SH with 25 mol% PI; mol% refer to the total quantity of thiols). Gelation was monitored by in-situ photo-rheology (UV, 17 mW/cm^2 light intensity, on between 30 and 150 s; frequency of 1 Hz; strain of 0.4 %). **B.** Corresponding shear storage moduli measured from frequency sweeps at 1 Hz and 0.4% strain. **C** & **D.** Imaging of hMSCs encapsulated and spreading in HA-SH hydrogels (10 mol% RGD, with respect to thiols) quantified by measurement of cell areas. ***, $p < 0.001$.

The impact of disulfide hydrogel compliance on hMSC spreading was comparable to that reported for HA hydrogels crosslinked by di-cysteine peptides via thiol-ene crosslinking[5], although cell spreading was typically observed at higher moduli. However, other parameters may play important role in regulating such behaviour. Hence, matrix viscoelasticity was found to modulate cell spreading in 3D matrices and MSCs were found to better spread in stiffer and more viscous non-degradable hydrogels[44]. In addition, matrix remodelling may play an impact on cell spreading and phenotype[22,

[45]. In photo-crosslinked disulfide hydrogels, stress relaxation was very limited and hydrogels displayed classic elastic profiles (Supplementary Figure S7). Therefore, cell spreading is proposed to mainly rely on degradation of the matrix. To investigate the impact of enzymatic degradation on this process, as is typical in the case of peptide-crosslinked hydrogels, or other natural matrices such as fibrin and collagen[5, 22], we allowed hMSCs to spread in disulfide hydrogels in the presence of the MMP inhibitor GM6001 10 μM and 25 μM[46]. We observed identical spreading, despite inhibition of enzymatic degradation (Supplementary Figure S10), consistent with the proposed degradation of disulfide networks by release of free thiols (perhaps including glutathione), although it is unclear what molecules specifically mediate this process. Matrix deposition may also help to promote the significant cell spreading observed in disulfide HA hydrogels. Indeed, we observed significant fibronectin deposition and early stages of fibrillation, indicating that cells are able to remodel their environment relatively fast in this system (Figure 7). Together, our results indicate that photo-crosslinked disulfide HA hydrogels may be interesting synthetic ECM candidates for the modulation of cell spreading and matrix remodelling for in vitro models and soft tissue engineering.

Conclusion

The ability to remodel synthetic hydrogels with external stimuli is a particularly interesting feature for the design of dynamic scaffolds for tissue engineering and advanced in vitro models. Synthetic extracellular matrix should allow the initial adhesion and spreading of cells and provide cues that help regulating their phenotype to promote regeneration of tissues needing repair, or the formation of organoids and organotypic structures mimicking tissue function in vitro. The ability to tune remodeling via light or the diffusion of small molecules will enable the control of cell spreading and tissue development in vitro, but will also allow the regulation of tissue remodeling in vivo. To this aim, strategies that enable the simple and affordable functionalization of approved soft scaffolds for hydrogel design is essential. The photo-crosslinking of thiolated HA developed in this study and the ability to remodel the resulting networks with light and small molecule diffusion demonstrate that simple chemical strategies towards such responsive materials can be implemented and may even be clinically viable. We also demonstrate that such materials are inherently cell remodellable, without the introduction of additional cell degradable moieties, and promote fast spreading of 3D embedded cells, independent of enzymatic degradation. This could be combined to enzymatic degradation and

the regulation of viscoelastic behavior of hydrogels (e.g. via physical crosslinks) to introduce complementary remodeling elements allowing to control tissue formation and regeneration. In this respect, better understanding the chemical processes controlling disulfide photo-remodeling will be particularly interesting to enhance the efficiency of associated processes and the control of their rates.

Associated Content

Supporting Information

The Supporting Information is available free of charge at https://pubs.acs.org/doi/.

^{1}H NMR of HA-SH, additional rheology data, calibration for mass spectrometry and Ellman's assay, additional mass spectrometry data, representative AFM indentation traces, cell viability data and corresponding microscopy images, cell spreading data and corresponding fluorescence microscopy images and fluorescence microscopy images taken to investigate the impact of inhibitors on cell spreading.

Acknowledgments

This work was supported by China Scholarship Council (grant no 201506550007) and from the European Research Council (ProLiCell, 772462).

References

1. Chaudhuri, O.; Koshy, S. T.; Branco da Cunha, C.; Shin, J.-W.; Verbeke, C. S.; Allison, K. H.; Mooney, D. J., Extracellular matrix stiffness and composition jointly regulate the induction of malignant phenotypes in mammary epithelium. *Nat. Mater.* **2014,** *13*, 970-978.
2. Loessner, D.; Rizzi, S. C.; Stok, K. S.; Fuehrmann, T.; Hollier, B.; Magdolen, V.; Hutmacher, D. W.; Clements, J. A., A bioengineered 3D ovarian cancer model for the assessment of peptidase-mediated enhancement of spheroid growth and intraperitoneal spread. *Biomaterials* **2013,** *34*, 7389-7400.
3. DeForest, C. A.; Tirrell, D. A., A photoreversible protein-patterning approach for guiding stem-cell fate in three-dimensional gels. *Nat. Mater.* **2015,** *14*, 523-531.
4. Chaudhuri, O.; Gu, L.; Darnell, M.; Klumpers, D.; Bencherif, S. A.; Weaver, J. C.; Huebsch, N.; Mooney, D. J., Substrate stress relaxation regulates cell spreading. *Nat. Commun.* **2015,** *6*, 6364.
5. Khetan, S.; Guvendiren, M.; Legant, W. R.; Cohen, D. M.; Chen, C. S.; Burdick, J. A., Degradation-mediated cellular traction directs stem cell fate in covalently crosslinked three-dimensional hydrogels. *Nat. Mater.* **2013,** *12*, 458-465.
6. Gjorevski, N.; Sachs, N.; Manfrin, A.; Giger, S.; Bragina, M. E.; Ordonez-Moran, P.; Clevers, H.; Lutolf, M. P., Designer matrices for intestinal stem cell and organoid culture. *Nature* **2016,** *539*, 560-564.
7. Tibbitt, M. W.; Anseth, K. S., Hydrogels as extracellular matrix mimics for 3D cell culture. *Biotech. Bioeng.* **2009,** *103* (4), 655-663.
8. Patterson, J.; Hubbell, J. A., Enhanced proteolytic degradation of molecularly engineered PEG hydrogels in response to MMP-1 and MMP-2. *Biomaterials* **2010,** *31*, 7836-7845.
9. Macdougall, L. J.; Perez-Madrigal, M. M.; Arno, M. C.; Dove, A. P., Nonswelling thiol-yne cross-linked hydrogel materials as cytocompatible soft tissue scaffolds. *Biomacromolecules* **2018,** *19*, 1378-1388.
10. Nair, D. P.; Podgorski, M.; Chatani, S.; Gong, T.; Xi, W.; Fenoli, C. R.; Bowman, C. N., The thiol-Michael addition click reaction: a powerful and widely used tool in materials chemistry. *Chem. Mater.* **2014,** *26*, 724-744.
11. DeForest, C. A.; Polizzotti, B. D.; Anseth, K., Sequential click reactions for synthesizing and patterning three-dimensional cell microenvironments. *Nat. Mater.* **2009,** *8* (8), 659-664.
12. deForest, C. A.; Anseth, K. S., Cytocompatible click-based hydrogels with dynamically tunable properties through orthogonal photoconjugation and photocleavage reactions. *Nat. Chem.* **2011,** *3*, 925-931.
13. Fairbanks, B. D.; Schwartz, M. P.; Halevi, A. E.; Nuttelman, C. R.; Bowman, C. N.; Anseth, K. S., A versatile synthetic extracellular matrix mimic via thiol-norbornene photopolymerization. *Adv. Mater.* **2009,** *21*, 5005-5010.
14. Colak, B.; Da Silva, J. C. S.; Soares, T. A.; Gautrot, J. E., Impact of the molecular environment on thiol-ene coupling for biofunctionalization and conjugation. *Bioconj. Chem.* **2016,** *27* (9), 2111-2123.
15. Khetan, S.; Katz, J. S.; Burdick, J. A., Sequential crosslinking to control cellular spreading in 3-dimensional hydrogels. *Soft Matter* **2009,** *5*, 1601-1606.
16. Sawicki, L. A.; Kloxin, A. M., Design of thiol-ene photoclick hydrogels usin facile techniques for cell culture applications. *Biomater. Sci.* **2014,** *2*, 1612-1626.
17. Fu, Y.; Xu, K.; Zheng, X.; Giacomin, A. J.; Mix, A. W.; Kao, W. J., 3D cell entrapment in

crosslinked thiolated gelatin-poly(ethylene glycol) diacrylate hydrogels. *Biomaterials* **2012,** *33*, 48-58.
18. Trappmann, B.; Baker, B. M.; Polacheck, W. J.; Choi, C. K.; Burdick, J. A.; Chen, C. S., Matrix degradability controls multicellularity of 3D cell migration. *Nat. Commun.* **2017,** *8*, 371.
19. Grube, S.; Oppermann, W., Inhomogeneity in hydrogels synthesized by thiol-ene polymerization. *Macromolecules* **2013,** *46*, 1948-1955.
20. Burdick, J. A.; Prestwich, G. D., Hyaluronic Acid Hydrogels for Biomedical Applications. *Adv. Mater.* **2011,** *23*, H41-H56.
21. Xu, X.; Jha, A. K.; Harrington, D. A.; Farach-Carson, M. C.; Jia, X., Hyaluronic acid-based hydrogels: from a natural polysaccharide to complex networks. *Soft Matter* **2012,** *8*, 3280-3294.
22. Loebel, C.; Mauck, R. L.; Burdick, J. A., Local nascent protein deposition and remodelling guide mesenchymal stromal cell mechanosensing and fate in three-dimensional hydrogels. *Nat. Mater.* **2019,** *18*, 883-891.
23. Lee, H. J.; Fernandes-Cunha, G. M.; Myung, D., In situ-forming hyaluronic acid hydrogel through visible light-induced thiolene reaction. *Reactive Funct. Polym.* **2018,** *131*, 29-35.
24. Asim, M. H.; Silberhumer, S.; Shahzadi, I.; Jalil, A.; Matuszczak, B.; Bernkop-Schnürch, A., S-protected thiolated hyaluronic acid: In-situ crosslinking hydrogels for 3D cell culture scaffold. *Carbohydrate Polym.* **2020,** *237*, 116092.
25. Rosales, A. M.; Vega, S. L.; DelRio, F. W.; Burdick, J. A.; Anseth, K. S., Hydrogels with reversible mechanics to probe dynamic cell microenvironments. *Angew. Chem., Int. Ed.* **2017,** *56*, 12132-12136.
26. Shu, X. Z.; Liu, Y.; Luo, Y.; Roberts, M. C.; Prestwich, G. D., Disulfide cross-linked hyaluronan hydrogels. *Biomacromolecules* **2002,** *3*, 1304-1311.
27. Zhang, G.; Liu, J.; Yang, Q.; Zhuo, R.; Jiang, X., Disulfide-containing brushed polyethylenimine derivative synthesized by click chemistry for nonviral gene delivery. *Bioconj. Chem.* **2012,** *23*, 1290-1299.
28. Cerritelli, S.; Velluto, D.; Hubbell, J. A., PEG-SS-PPS: Reduction-sensitive disulfide block copolymer vesicles for intracellular drug delivery. *Biomacromolecules* **2007,** *8*, 1966-1972.
29. Fairbanks, B. D.; Singh, S. P.; Bowman, C. N.; Anseth, K. S., Photodegradable, photoadaptable hydrogels via radical-mediated disulfide fragmentation reaction. *Macromolecules* **2011,** *44*, 2444-2450.
30. Bermejo-Velasco, D.; Azemar, A.; Oommen, O. P.; Hilborn, J.; Varghese, O. P., Modulating thiol pKa promotes disulfide formation at phsyiological pH: an elegant strategy to design disulfide cross-linked hyaluronic acid hydrogels. *Biomacromolecules* **2019,** *20*, 1412-1420.
31. Murphy, R. D.; in het Panhuis, M.; Cryan, S.-A.; Heise, A., Disulphide crosslinked star block copolypeptide hydrogels: influence of block sequence order on hydrogel properties. *Polym. Chem.* **2018,** *9*, 3908-3916.
32. Li, L.; Feng, W.; Welle, A.; Levkin, P. A., UV-induced disulfide formation and reduction for dynamic photopatterning. *Angew. Chem., Int. Ed.* **2016,** *55* (44), 13765-13769.
33. Oliver, W. C.; Pharr, G. M., An improved technique for determining hardness and elastic modulus using load and displacement sensing indentation experiments. *J. Mater. Res.* **1992,** *7* (1), 1564-1583.
34. Megone, W.; Roohpour, N.; Gautrot, J. E., Impact of surface adhesion and sample heterogeneity on the multiscale mechanical charcaterisation of soft biomaterials. *Sci. Rep.* **2018,** *8*, 6780.
35. Brown, T. E.; Anseth, K. S., Spatiotemporal hydrogel biomaterials for regenerative medicine.

Chem. Soc. Rev. **2017,** *46* (21), 6532-6552.
36. Kloxin, A. M.; Kasko, A. M.; Salinas, C. N.; Anseth, K., Photodegradable hydrogels for dynamic tuning of physical and chemical properties. *Science* **2009,** *324*, 59-63.
37. Phadke, A.; Zhang, C.; Arman, B.; Hsu, C.-C.; Mashelkar, R. A.; Lele, A. K.; Tauber, M. J.; Arya, G.; Varghese, S., Rapid self-healing hydrogels. *Proc. Natl. Acad. Sci.* **2012,** *109* (12), 4383-4388.
38. Imbernon, L.; Oikonomou, E. K.; Norvez, S.; Leibler, L., Chemically crosslinked yet reprocessable epoxidized natural rubber via thermo-activated disulfide rearrangements. *Polym. Chem.* **2015,** *6*, 4271.
39. Yang, W. J.; Tao, X.; Zhao, T.; Weng, L.; Kang, E.-T.; Wang, L., Antifouling and antibacterial hydrogel coatings with self-healing properties based on a dynamic disulfide exchange reaction. *Polym. Chem.* **2015,** *6*, 7027-7035.
40. Meister, A.; Anderson, M. E., Glutathione. *Ann. Rev. Biochem.* **1983,** *52*, 711-760.
41. Huebsch, N.; Arany, P. R.; Mao, A. S.; Shvartsman, D.; Ali, O. A.; Rivera-Feliciano, J.; Mooney, D. J., Harnessing tractio-mediated manipulation of the cell/matrix interface to control stem-cell fate. *Nat. Mater.* **2010,** *9*, 518-526.
42. Ruskowitz, E. R.; DeForest, C. A., Proteome-wide Analysis of Cellular Response to Ultraviolet Light for Biomaterial Synthesis and Modification. *ACS Biomater. Sci. Eng.* **2019,** *5* (5), 2111-2116.
43. Bensaid, W.; Triffitt, J. T.; Blanchat, C.; Oudina, K.; Sedel, L.; Petite, H., A biodegradable fibrin scaffold for mesenchymal stem cell transplantation. *Biomaterials* **2003,** *24*, 2497-2502.
44. Chaudhuri, O.; Gu, L.; Klumpers, D.; Darnell, M.; Bencherif, S. A.; Weaver, J. C.; Huebsch, N.; Lee, H.-P.; Lippens, E.; Duda, G. N.; Mooney, D. J., Hydrogels with tunable stress relaxation regulate stem cell fate and activity. *Nat. Mater.* **2016,** *15*, 326-334.
45. Ferreira, S. A.; Motwani, M. S.; Faull, P. A.; Seymour, A. J.; Yu, T. T. L.; Enayati, M.; Taheem, D. K.; Salzlechner, C.; Haghighi, T.; Kania, E. M.; Oommen, O. P.; Ahmed, T.; Loaiza, S.; Parzych, K.; Dazzi, F.; Varghese, O. P.; Festy, F.; Grigoriadis, A. E.; Auner, H. W.; Snijders, A. P.; Bozec, L.; Gentleman, E., Bi-directional cell-pericellular matrix interactions direct stem cell fate. *Nat. Commun.* **2018,** *9*, 4049.
46. Galardy, R. E.; Cassabonne, M. E.; Giese, C.; Gilbert, J. H.; Lapierre, F.; Lopez, H.; Schaefer, M. E.; Stack, R.; Sullivan, M.; Summers, B.; Tressler, R.; Tyrrell, D.; Wee, J.; Allen, S. D.; Castellot, J. J.; Barletta, J. P.; Schultz, G. S.; Fernandez, L. A.; Fisher, S.; Cui, T.-Y.; Foellmer, H. G.; Grobelny, D.; Holleran, W. M., Low molecular weight inhibitors in corneal ulceration. *Ann. N Y Acad. Sci.* **1994,** *732*, 315-323.